The Numerical Modeling and Measurement of Demagnetization Effect in Bulk YBCO Superconductors Subjected to Transverse Field

Z. Hong, Ph. Vanderbemden, R. Pei, Y. Jiang, A. M. Campbell, and T. A. Coombs

Abstract—In this paper, the crossed field demagnetization effect of the bulk type-II superconducting materials in a variety of external magnetic field condition has been investigated both numerically and experimentally. A melt-textured YBCO bulk sample was magnetized along the axial direction and after that a transverse field perpendicular to the central axis applied. The collapse of the original trapped field was measured using a *Quantum Design Physical Property Measurement System*. A numerical solver based on critical state model is proposed to simulate the measured results.

Index Terms—Bulk superconductor, critical state model, crossed field effect, finite element method, numerical modeling.

I. INTRODUCTION

THE potential of bulk melt-processed YBCO single domains to trap significant magnetic field at 77 K makes them particularly attractive for a variety of engineering applications including superconducting magnets, magnetic bearings and motors [1], [2]. Before such devices can be created, the characteristics of these trapped field magnets need to be well understood. A major cause of concern is the phenomenon of magnetization decay, which has been observed when the material is subjected to magnetic fields in a direction transverse to the original magnetization, result in magnets losing their magnetization and thus becoming worthless in applications. In spite of having been investigated for more than three decades, the subject remains a very intriguing topic for which many experimental facts are still far from being understood. In particular, we need to know whether large numbers of cycles of the crossed field lead eventually to total demagnetization, as suggested by some experiments and theories [3], or the decay of the magnetization ceases at a useful value as predicted by theories based on the critical state model [4], [5]. In this paper, a melt-textured YBCO bulk sample was magnetized along the axial direction and after that a transverse field perpendicular to the central axis applied. The collapse of the original trapped field was measured using a *Quantum Design Physical Property*

Measurement System (PPMS) and found that the decay of the magnetization can be fitted using a power law $M \sim N^{\alpha}$ where N is the number of the transverse field sweeps. A two dimensional numerical model based on a set of Maxwell's equations is proposed to simulate the electromagnetic behavior of the YBCO bulks. The model assumes a field dependent J_c and is used with $E - J$ power constitutive law; it can qualitatively reproduce the experimental results and help to investigate the current and field distributions throughout the cross sectional area of the sample.

II. NUMERICAL MODEL

The numerical solver of the critical state used in this paper is based on a set of Maxwell's equations using magnetic field H_x and H_y as the knowns. The equations are incorporated with a commercial finite element software *Comsol Multiphysics*.

According to Faraday's Law,

$$\nabla \times \mathbf{E} = -\mu_0 \mu_r \frac{\partial \mathbf{H}}{\partial t} \tag{1}$$

The magnetic flux is flowing in the x-y plane and the magnetic field is used as the dependent variable $\mathbf{H} = [H_x H_y]$ representing the components of the magnetic field in the x and y directions. The induced electric field and the current density only have the components in the z-direction. So $E = E_{sc\_z}$ and $J = J_{sc\_z}$. The electrical behavior of the superconducting material is represented by the $E - J$ power law. In this case, it is expressed as:

$$E_{sc\_z} = E_0 \left(\frac{J_{sc\_z}}{J_c(B)} \right)^n \tag{2}$$

where J_c is the critical current density (defined with the standard 1 μV/cm electric field criterion). $E_0 = 1 \times 10^{-4}$ V/m and the value of "n" is determined by the characteristics of the superconducting materials.

According to Ampere's law:

$$\nabla \times H = J \tag{3}$$

Since J_{sc_z} only has the component in the z-direction, Ampere's law in this case is expressed as:

$$J_{sc\_z} = \frac{\partial H_y}{\partial x} - \frac{\partial H_x}{\partial y} \tag{4}$$
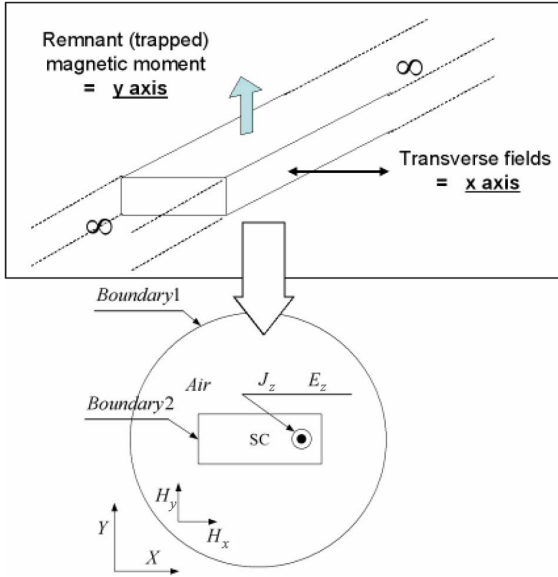
Fig. 1.   Diagram of model, subdomains and boundaries. The magnetic field is in the x-y plane and the critical current density J_z and the induced electric field E_z are in the z-direction.
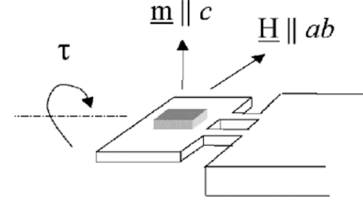

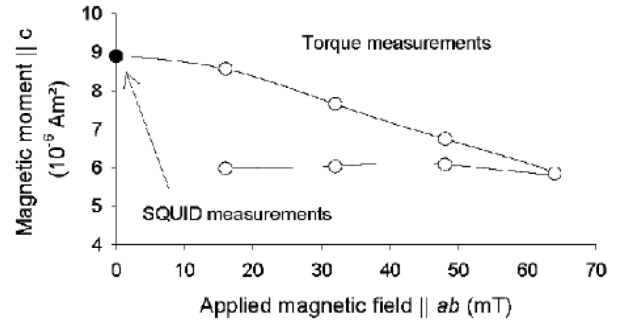Fig. 2.   Schematic illustration of the sample mounted on the platform used for torque measurements.

Fig. 3.   Magnetic moment $\parallel c$-axis during the application of one sweep of transverse field $\parallel ab$. Black symbol: initial trapped magnetic moment without transverse field. White symbols: data determined from magnetic torque measurements.

Substitution of (2) and (4) into (1) gives two coupled equations:

$$\partial \left(E_0 \left(\frac{\frac{\partial H_y}{\partial x} - \frac{\partial H_x}{\partial y}}{J_c(B)} \right)^n \right) \bigg/ \partial y = -\mu_0 \mu_r \frac{\partial H_x}{\partial t} \quad (5)$$

$$-\partial \left(E_0 \left(\frac{\frac{\partial H_y}{\partial x} - \frac{\partial H_x}{\partial y}}{J_c(B)} \right)^n \right) \bigg/ \partial x = -\mu_0 \mu_r \frac{\partial H_y}{\partial t} \quad (6)$$

Equations (5) and (6) include two PDEs and two scalar dependent variables H_x and H_y. Combining this with suitable boundary conditions, they can be solved with FEM software.

On the outer boundary of the non-superconducting region (boundary 1 in Fig. 1), a Dirichlet boundary condition can be set up as:

$$\begin{cases} H_x = f_x(t) \\ H_y = f_y(t) \end{cases} \quad (7)$$

Where $f_x(t)$ and $f_y(t)$ are functions that describes how the external field in the x and y directions vary with time.

III. EXPERIMENT

Small sample of bulk melt-processed single domain YBCO with an aspect ratio of ~1:3 (typical size $0.8 \times 0.8 \times 0.25 \text{ mm}$) were cut from the parent single domain using a wire saw. These samples were characterized magnetically for applied field conditions of $H \parallel ab$ and $H \parallel c$ at $T = 77$ K using a Quantum Design SQUID Magnetic Property Measurement System (MPMS). The full penetration fields along ab plane and c axis are 64 mT and 74 mT respectively.

Measurements of the YBCO samples in the crossed-field configuration were carried out using magnetic torque magnetometry in PPMS. In this case, the magnetic torque can be expressed as;

$$\underline{\tau} = \underline{m_c} \times \mu_0 \underline{H_{ab}} \quad (7.1)$$

The variation of magnetic moment m_c vs. the applied field H_{ab} can be determined from the measured torque by $m_c(H_{ab}) = \tau(H_{ab})/(\mu_0 H_{ab})$, since m_c and H_{ab} are mutually orthogonal, as shown in Fig. 2. This technique is particularly convenient for determining accurately the magnetic moment of small-size superconductors subjected to crossed fields.

However, one constraint of the method is that the measurements must always be performed in the presence of a small but finite transverse field H_{ab}. As shown in Fig. 3, the measured $m_c(H_{ab})$ data obtained by torque measurements agree perfectly with the initial value of magnetic moment determined by SQUID magnetometry in the absence of a transverse field.

In all experiments, the melt-processed sample was initially magnetized parallel to the c-axis by field cooling (FC) down to $T = 77$ K in an applied magnetic flux density of 0.5 T. The field amplitude was intentionally much larger than the full-penetration field of the sample ($\mu_0 H_p = 64 \text{ mT}$) to ensure that the maximum (trapped) magnetic moment m_c is achieved [6]. A constant time interval of approximately 5 minutes was allowed for magnetic relaxation following the removal of the applied (c-axis) field [7]. A transverse magnetic field H_{ab} was then applied parallel to the ab plane of the sample and the magnetic
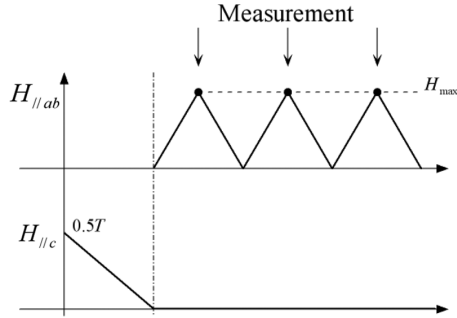
Fig. 4. Schematic illustration and the sequences of magnetic fields applied to the sample.
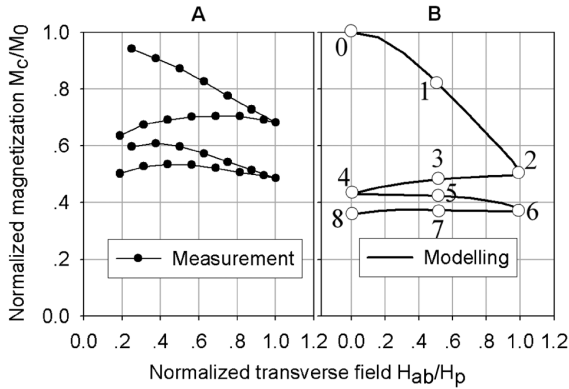

Fig. 5. Measured and modeled magnetization ∥ c during the application of two cycles of transverse field ∥ ab. The magnetization is normalized with respect to its initial value M_0. The transverse field is normalized with respect to the full penetration field H_p.

Fig. 6. Modeled data of the current density distribution $J_{z\_sc}(\mathrm{x},\mathrm{y})$ within the cross-section of the sample during one cycle of the transverse magnetic field of amplitude 0.5 H_p. The number of images correspond to the time steps listed in Fig. 5(b).

$M_\mathrm{c}(H_\mathrm{ab})$ curves are remarkably similar to the experimental data. In particular, the $M_\mathrm{c}(H_\mathrm{ab})$ segments that correspond to sweeps from $+H_\mathrm{max}$ to 0 and from $-H_\mathrm{max}$ to 0 are nearly horizontal, showing clearly that the remanent magnetization is affected only weakly by the transverse field in this regime.

Fig. 6 shows the current distribution modeled within the sample cross-section at several selected times during the first and the second transverse field cycle for transverse field amplitude of H_p. The images correspond to the time steps listed in Fig. 5(b). The surface plot represents the current density; the light region stands for the positive current and the dark region stands for the negative current. Image 0 shows the current distribution that gives rise to a positive trapped magnetization (i.e. $M_\mathrm{c} > 0$). The magnitude of the current density is not uniform. This arises from the $J_\mathrm{c}(B)$ dependence. The application of a positive transverse field $H_\mathrm{ab} > 0$ leads to a reversal of the current density in the top-left and bottom-right regions of the sample, as shown in Image 1. The consequence is that both upper and lower layers of the sample no longer contribute efficiently to the c-axis magnetization M_c. Increasing the field (Image 2) increases the distortion of the current distribution. On lowering the field (Images 3 and 4), the shielding currents in the top and bottom layers change their sign, as required for shielding the decreasing applied field $\mathrm{d}H_\mathrm{ab}/\mathrm{dt} < 0$. However the current distribution in the central horizontal layer of the sample remains unaffected. The corresponding decay of M_c is therefore very small, as observed in Fig. 5.

B. Large Number of Sweeps of Transverse Field

After the sample is magnetized by field cooling, a transverse field demagnetization sequence is cycled by 120 times between 0 and $+H_\mathrm{max}$. This measurement is taken with H_max equals to 0.25 and 0.5 full penetration field (H_p) respectively. The influence of this large number of transverse field sweeps on the remanent magnetization of the sample is examined. The experimental results are presented in Fig. 7(a), which shows the normalized magnetization M_c measured by $PPMS$ at the each moment $H_\mathrm{ab} = H_\mathrm{max}$. Successive cycles cause the magnetization to decrease by smaller and smaller amounts, as illustrated by the log-log plot of the data. The striking feature of Fig. 7 is that the induction M_c does not appear to saturate, even after a large number of field sweeps. Indeed, the M_c vs. cycle number N curves can be fitted using a power law $M_\mathrm{c} \sim \mathrm{N}^{-\alpha}$, as a straight line in log-log plot, with the exponent α being an increasing function of the transverse field amplitude H_max.

Similar experimental conditions were used in the model, and the results are shown in Fig. 7(b). Good agreement between the experimental data and a power law fit is observed over the whole

torque recorded, as illustrated schematically in Fig. 2 and Fig. 4.

IV. RESULTS

A. Demagnetization in the First and Second Cycle

Fig. 5(a) shows the influence of transverse magnetic field sweeps H_ab on the trapped magnetization M_c (∥ c-axis) measured by a $PPMS$. The magnetization is normalized with respect to its initial value, M_0, measured by SQUID, whereas the transverse field is normalized with respect to the full-penetration field H_p in the ab direction. The experimental data display the remaining M_c after one cycle is found to be $\sim 0.62 M_0$. Secondly, the consistent decreases in M_c observed when H_ab is swept from 0 to $+H_\mathrm{max}$ are generally much larger than the decrease in magnetization caused by sweeps from $+H_\mathrm{max}$ to 0. Thirdly, the results displayed in Fig. 5(a) also show that the second cycle of the transverse field causes less magnetization decrease than that of the first cycle

Fig. 5(b) shows the results of the modeling, corresponding to the experimental conditions described above. From a quantitative point of view, the induction decays resulting from one complete oscillation of the transverse field are found to be much more pronounced than those measured experimentally: after one cycle of H_ab, the remaining M_c is only $\sim 0.45 M_0$, compared to $\sim 0.62 B_0$ for the experimental data. These differences are due to the differences between the model and experimental geometries. From a qualitative point of view, however, the modeled
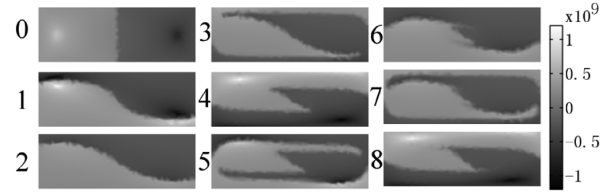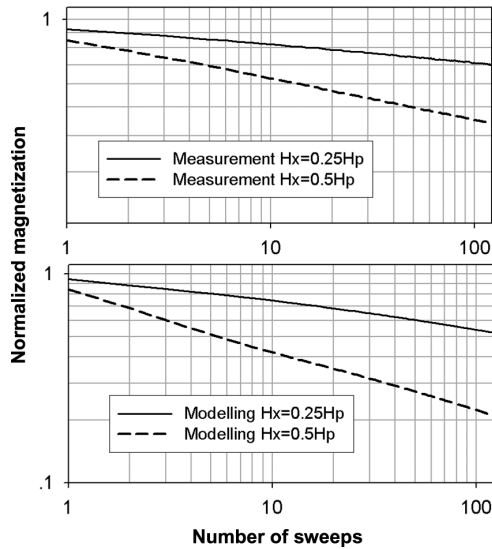
Fig. 7. Log-log plot of the measured and modeled magnetization at each peak positive transverse field for two different transverse field sweep amplitudes.
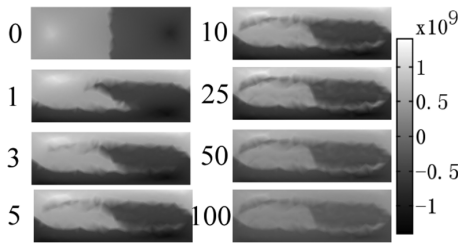

Fig. 8. Current distributions on the cross section of the sample at the end of the corresponding number of sweeps.

range of N $(1 < N < 100)$. As is observed experimentally, the remanent induction continues to decrease after 100 sweeps, and no saturation occurs.

The evolution of the current distribution over 100 sweeps is calculated by the model and shown in Fig. 8. The images are the current distribution on the cross section of the sample at the moment of the end of the 1st, 3rd, 5th, 10th, 25th, 50th and 100th sweep. As can be seen from the images, the current profile changes during the initial sweeps and reaches a relatively balanced distribution at the 10th sweep. These current profiles are made up of two regimes: regime 1 is two horizontal layers carrying positive and negative current located at the top and the bottom of the sample; regime 2 is the central area in which the original current distribution remains. The horizontal layers on the top and bottom no longer contribute to the c-axis magnetization. The forming of this current distribution gives the decay of M_c in the initial a few sweeps. After the 10th sweep, the magnitude of the current changes rather than the distribution.

There are two characteristic changes to the magnitude of the current; the first one is that the value of the current in regime 1 increases with a few sweeps (images 1–5) and decrease afterwards (images 10–100); the other is the magnitude of the current in the central region (regime 2) decreases. A reasonable explanation of this phenomenon is that the applied transverse field always tries to destroy the initially trapped magnetization, either by taking over the space which is originally occupied by

the current contributed to c-axis magnetization (regime 2), or by reducing the magnitude of that current. However the transverse field would not affect the magnitude of the current in the top and bottom layers (regime 1) which contribute to ab-axis magnetization. In the mean while, $J_c(\mathrm{B})$ increases as the local magnetic flux density decreases, that is the reason of the increase of the magnitude of the current density in regime 1. The exponential decay of magnetization against the number of sweeps is determined mainly by the decrease of the magnitude of current density in regime 2.

An important argument which must be clarified is whether this exponential decay of magnetization is due to the repeated application of the transverse field or just the normal flux creep relaxation. The contribution of the decay arising from flux-creep effects during a crossed field experiment can be estimated by the model. To be consistent with the experiment, the present model allows a time of 300 s to elapse after the magnetization process. The magnetization decreases by approximately 29% during this period and then by a further 0.13% during the application of one full cycle of the transverse field. Considering the period for a large number (100) of transverse field sweeps, the corresponding decrease due to flux creep is 4.5%. Such values are much smaller then the decay in magnetization observed in Fig. 7(a) in which the magnetizations decrease for 30% and 55% for the two curves at the end of the 100th sweep. The discussion above shows that the decay of magnetization in Fig. 7 is mainly due to the crossed field effect.

V. CONCLUSION

The study in this paper focuses on the magnetization decay in a superconductor pre-magnetized along its shortest direction (c-axis) and then subjected to a series of transverse field cycles. The model shows that the suppression of magnetization results primarily from the modification of the current distribution in layers of the sample that are perpendicular to the direction of the pre-magnetization. The results obtained in the present study also allow significant conclusions to be drawn that a large number of sweeps in transverse field causes the magnetic induction to decrease continuously following a power law whose exponent is related to the sweep amplitude. The model proposed in this study offers a simple way of predicting the electromagnetic behavior of YBCO pellets subjected to crossed magnetic fields.

REFERENCES

[1] A. M. Campbell and D. A. Cardwell, "Bulk high temperature superconductors for magnet applications," *Cryogenics*, vol. 37, 1997.
[2] T. A. Coombs, A. M. Campbell, R. Storey, and R. Weller, "Superconducting magnetic bearings for energy storage flywheels," *IEEE Trans. Appl. Supercond.*, vol. 9, 1999.
[3] P. Vanderbemden, Z. Hong, T. A. Coombs, S. Denis, M. Ausloos, J. Schwartz, I. B. Rutel, N. H. Babu, D. A. Cardwell, and A. M. Campbell, "Behavior of bulk high-temperature superconductors of finite thickness subjected to crossed magnetic fields: Experiment and model," *Physical Review B*, vol. 75, p. 174515, 2007.
[4] L. M. Fisher *et al.*, "Superposition of currents in hard superconductors placed into crossed ac and dc magnetic fields," *Solid State Commun.*, vol. 97, 1996.
[5] L. M. Fisher *et al.*, "Collapse of the magnetic moment in a hard superconductor under the action of a transverse ac magnetic field," *Physica C*, vol. 278, 1997.
[6] D. A. Cardwell *et al.*, "Round robin measurements of the flux trapping properties of melt processed Sm-Ba-Cu-O bulk superconductors," *Physica C*, vol. 623, 2004.
[7] P. W. Anderson and Y. B. Kim, "Hard Superconductivity: Theory of the motion of Abrikosov flux lines," *Review of Modern Physics*, vol. 129, pp. 528–536, 1964.